SEISMIC PERFORMANCE OF MULTI-STORY STRUCTURES EQUIPPED WITH UPLIFT-RESTRAINED OPRCB ISOLATORS

Mahmood HOSSEINI
Associate Professor, Structural Engineering Research Center,
the International Institute of Earthquake Engineering and Seismology (IIEES), Tehran, Iran
hosseini@iiees.ac.ir

Sadegh MAHMOUDKHANI
Adjunct Lecturer, Islamic Azad University, Tehran, Iran
s.mahmoudkhani@srbiau.ac.ir

Keywords: Base Isolation, Lagrange Equations of Motion, Time History Analysis, Inter-Story Drift, Floor Absolute Accelerations

ABSTRACT

Orthogonal Pairs of Rollers on Concave Beds (OPRCB) isolators are a recently introduced seismic isolating system which in their original form are weak against uplift. In this study, the use of Uplift-Restrained OPRCB (UR-OPRCB) isolators for seismic response reduction of multi story buildings is presented, in which three regular square plan buildings with 3, 6 and 9 stories, all having nine columns in their plan were considered. In this way the tendency of building to rocking motion and the resulting compressional and tensile axial forces in the building column, leading to additional compressive force between roller and their beds or uplift of isolator plates can be taken into account. A series of time history analysis have been conducted for each of the considered buildings. Results show that using UR-OPRCB isolators can reduce the maximum story drift values around 20%, and the maximum absolute acceleration values around 60% in average. In case of some earthquake records slight increase in the maximum story drift values is observed which can be due to the relatively high energy of those earthquakes in the range of long periods.

INTRODUCTION

Among various seismic isolation techniques rolling-based isolation has been acknowledged by several researchers and practicing engineers because of their ease of manufacturing and low-cost construction. Equations of motion for this type of isolators have been derived for 2D state (one horizontal direction of motion are considered for rollers) for either rollers with circular section (Jangid, 1995), or with non-circular section (Londhe, 1999) on flat beds. Also rollers on non-flat beds such as V-shaped (Tsai et al., 2007; Ou et al., 2010) and eccentric rollers (Chung et al., 2009) have been studied. Furthermore, they have been studied as pair of rollers on concave beds (OPRCB) (Hosseini and Soroor, 2011) or V-shape beds (Wang et al., 2014) all in the state of one directional motion of rollers. Hosseini and Soroor (2013) stated that rolling-based isolators are weak against uplift, and that in case of relatively tall buildings, particularly when subjected to near-fault earthquakes with high vertical ground acceleration, the rolling isolators lose their proper function due to uplift forces which result in separation of columns bases from rollers.

One possible way to prevent OPRCB isolators against uplift phenomenon is adding some specific parts to the isolators between the upper and lower plates to keep them and rollers all in touch together all the time during earthquake. Mahmoudkhani (2013) proposed a kind of restrainers for OPRCB isolators by using U-shaped elements, and developed the equations of motion of OPRCB isolators in 3D state considering both horizontal components as well as the vertical component of ground motion. In that study two directional motion of rollers and the effect of forces acting between the U-shape elements and lower, middle, and upper plates of OPRCB isolators during uplift have been considered. Mahmoudkhani (2013) finally has derived the required formulations of a single Uplift-Restrained OPRCB (UR-OPRCB) isolator. In this study employing the UR-OPRCB for seismic isolation of multi-story buildings is discussed.

THE USE OF UR-OPRCB ISOLATORS IN BASE ISOLATION OF MULTI-STORY BUILDING

Fig. 1 shows schematic 3D view of a set of UR-OPRCB isolator and the geometric features of one pair of rollers with their concave beds.

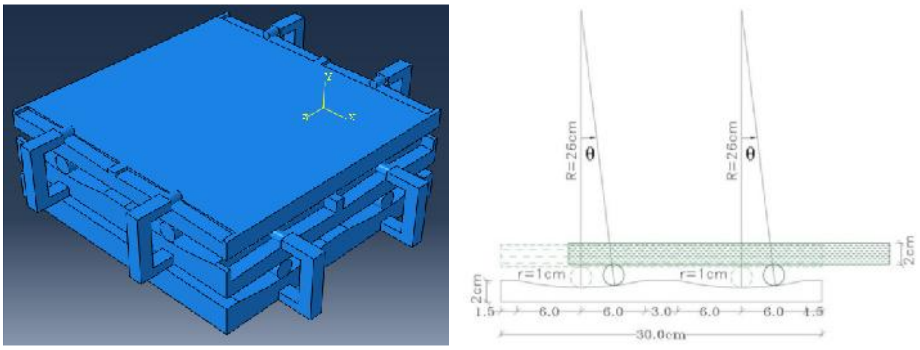

Figure 1. The complete set of UR- OPRCB isolator (left) (Mahmoudkhani, 2013), and geometric futures of its bed and middle plate and rollers (right) (Hosseini and Soroor, 2011)

To show how the UR-OPRCB isolators reduce the seismic response of multi-story buildings, a set of symmetrical buildings with square plan of 2 bays of equal spans in both directions were considered. These buildings all have 9 columns in their plans, which is the minimum number making it possible to observe the uplift effect on all types of middle, side and corner columns of the building (Fig. 2).

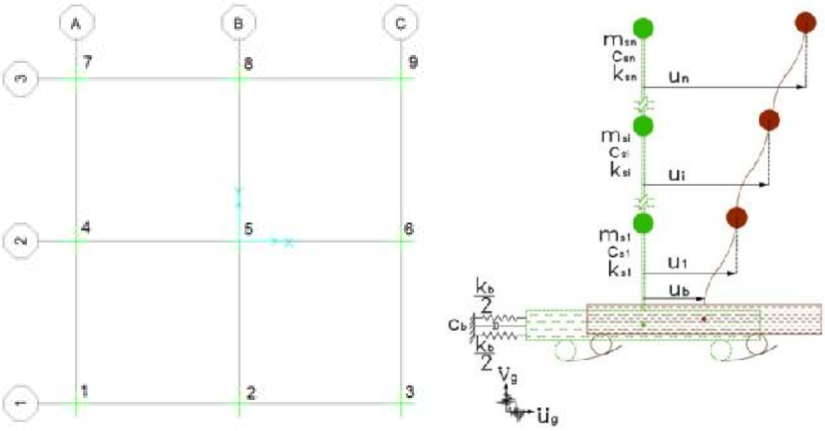

Figure 2. Typical plan of the studied buildings (right) (Mahmoudkhani, 2013), and their schematic dynamic model for one directional motion (left) (Hosseini and Soroor, 2013)

The schematic dynamic model of the buildings shown in Fig. 2(left) is used for developing the equations of motion of buildings in bidirectional states as presented in following section. To develop equations of motions of multi-story building equipped with UR-OPRCB isolators which have possibility of independent motion in two main horizontal directions, set of Lagrange Equations of motion were used, which can be stated for each degree of freedom *i* of the system, as:

$$\frac{d}{dt}\left(\frac{\partial T}{\partial \dot{q}_i}\right) - \frac{\partial T}{\partial q_i} + \frac{\partial V}{\partial q_i} = Q_i \tag{1}$$

in which *T* and *V* are, respectively, kinetic and potential energy terms of the system, which are expressed with respect to the independent variables of the system (q_i) which in case of the problem at hand include rotation of rollers in x and y directions (θ_x, θ_y) and displacement of the *i-th* story of the building in x and y direction with respect to the base (u_{ix}, u_{iy}), as:

$$T=\frac{1}{2}m_b(R-r)^2\left(\dot{\theta}_x^2\cos^4\frac{\theta_x}{2}+\dot{\theta}_y^2\cos^4\frac{\theta_y}{2}\right)+\frac{1}{2}\sum_{i=1}^{n}\left[m_i\left(\dot{u}_{ix}^2+\dot{u}_{iy}^2\right)\right]$$
$$+\frac{1}{2}m_t(R-r)^2\left(\dot{\theta}_x^2\sin^2\theta_x+\dot{\theta}_y^2\sin^2\theta_y\right) \tag{2}$$

$$V=\frac{1}{2}k_{bx}(R-r)^2(\theta_x+\sin\theta_x)^2+\frac{1}{2}k_{by}(R-r)^2(\theta_y+\sin\theta_y)^2$$
$$+m_tg(R-r)(2-\cos\theta_x-\cos\theta_y)+\frac{1}{2}\sum_{i=2}^{n}k_{ix}\left(u_{ix}-u_{(i-1)x}\right)^2+\frac{1}{2}\sum_{i=2}^{n}k_{iy}\left(u_{iy}-u_{(i-1)y}\right)^2$$
$$+\frac{1}{2}k_{1x}\left(u_{1x}-(R-r)(\theta_x+\sin\theta_x)\right)+\frac{1}{2}k_{1y}\left(u_{1y}-(R-r)(\theta_y+\sin\theta_y)\right) \tag{3}$$

where m_b, k_{bx} and k_{by} are respectively mass and stiffness coefficients of the base in x and y directions, m_t is the total mass of the building, m_i is the mass of the *i-th* story, and k_{ix} and k_{iy} are respectively stiffness coefficients of the story in x and y directions. In Eq. (1) Q_i is the non-conservative force which includes the effect of seismic forces as well as rolling friction and damping forces corresponding the *i-th* degree of freedom of the system. The variation of all non-conservative forces can be expressed as:

$$\delta W_{nc}=\left[-m_b\ddot{u}_{gx}-2c_{bx}(R-r)\dot{\theta}_x\cos^2\frac{\theta_x}{2}+c_{1x}\left(\dot{u}_{1x}-2(R-r)\dot{\theta}_x\cos^2\frac{\theta_x}{2}\right)\right](R-r)(1+\cos\theta_x)\delta\theta_x$$
$$+\left[-m_b\ddot{u}_{gy}-2c_{by}(R-r)\dot{\theta}_y\cos^2\frac{\theta_y}{2}+c_{1y}\left(\dot{u}_{1y}-2(R-r)\dot{\theta}_y\cos^2\frac{\theta_y}{2}\right)\right](R-r)(1+\cos\theta_y)\delta\theta_y$$
$$-\sum_{l=1}^{9}\left[heaviside(N_{2lx})\operatorname{sgn}(\dot{\theta}_x)F_{rlx}(R-r)\right]\delta\theta_x-\sum_{l=1}^{9}\left[heaviside(N_{2ly})\operatorname{sgn}(\dot{\theta}_y)F_{rly}(R-r)\right]\delta\theta_y$$
$$-m_t\ddot{v}_g(R-r)\sin\theta_x\delta\theta_x+\sum_{l=1}^{9}\left[\frac{heaviside(-N_{2lx})\operatorname{sgn}(\dot{\theta}_x)F_{rulx}(R-r)(1+\cos\theta_x)}{\cos\alpha_x}\right]\delta\theta_x$$
$$-m_t\ddot{v}_g(R-r)\sin\theta_y\delta\theta_y+\sum_{l=1}^{9}\left[\frac{heaviside(-N_{2ly})\operatorname{sgn}(\dot{\theta}_y)F_{ruly}(R-r)(1+\cos\theta_y)}{\cos\alpha_y}\right]\delta\theta_y$$
$$+\left[-m_1\ddot{u}_{gx}-c_{1x}\left(\dot{u}_{1x}-2(R-r)\dot{\theta}_x\cos^2\frac{\theta_x}{2}\right)+c_{2x}(\dot{u}_{2x}-\dot{u}_{1x})\right]\delta u_{1x}$$
$$+\left[-m_1\ddot{u}_{gy}-c_{1y}\left(\dot{u}_{1y}-2(R-r)\dot{\theta}_y\cos^2\frac{\theta_y}{2}\right)+c_{2y}(\dot{u}_{2y}-\dot{u}_{1y})\right]\delta u_{2x}$$
$$+\sum_{i=2}^{n}\left[-m_i\ddot{u}_{gx}-c_{ix}\left(\dot{u}_{ix}-\dot{u}_{(i-1)x}\right)+c_{(i+1)x}\left(\dot{u}_{(i+1)x}-\dot{u}_{ix}\right)\right]\delta u_{ix}$$
$$+\sum_{i=2}^{n}\left[-m_i\ddot{u}_{gy}-c_{iy}\left(\dot{u}_{iy}-\dot{u}_{(i-1)y}\right)+c_{(i+1)y}\left(\dot{u}_{(i+1)y}-\dot{u}_{iy}\right)\right]\delta u_{iy} \tag{4}$$

Heaviside and sgn in Eq. (4) are the well-known mathematical functions. In Eq. (4) α_x and α_y are, respectively, the amounts of rotation of the roller of U-shaped restrainers in x and y directions with respect to their initial positions, which are functions of θ_x or θ_y correspondingly (Mahmoudkhani, 2013). The rolling friction terms in Eq. (4) are given by either Eqs. (5) or (6) depending on whether the isolator is under compression or tension (uplift).

$$F_{rl(x,y)}=\mu_{r1l(x,y)}N_{1l(x,y)}+\mu_{r2l(x,y)}N_{2l(x,y)} \tag{5}$$

$$F_{rul(x,y)}=\mu_{r3l(x,y)}N_{3l(x,y)} \tag{6}$$

Eq. (5) gives the rolling resistance forces, either in x or y direction, as the product of the rolling resistance coefficients, $\mu_{r1l(x,y)}$ and $\mu_{r2l(x,y)}$ and their corresponding normal compressional forces between the rollers and the lower, middle, and upper plates, $N_{1(x,y)}$, $N_{2(x,y)}$. Also Eq. (6) gives the rolling resistance forces, either in x or y direction, as the product of the rolling resistance coefficient, $\mu_{r3l(x,y)}$ and the corresponding normal tensile forces (uplift) between the curved surfaces at the top of the upper plate and the rollers of the U-shaped restrainers, $N_{3(x,y)}$. Values of $N_{1(x,y)}$, $N_{2(x,y)}$ and $N_{3(x,y)}$ are given by:

$$N_{1l(x,y)} = \frac{N_{2l(x,y)}}{\cos\theta_{(x,y)} - \mu_{r1l(x,y)}\,\mathrm{sgn}\left(\dot{\theta}_{(x,y)}\right)\sin\theta_{(x,y)} + \tan\frac{\theta_{(x,y)}}{2}\sin\theta_{(x,y)}} \tag{7}$$

$$N_{2l(x,y)} = \frac{m_b}{4}\left[(R-r)\left(\ddot{\theta}_{(x,y)}\sin\theta_{(x,y)} + \dot{\theta}^2_{(x,y)}\cos\theta_{(x,y)} + \ddot{v}_g + g\right)\right] + P_l \tag{8}$$

$$N_{3l(x,y)} = \frac{\left|N_{2l(x,y)}\right|}{\cos\varphi_{(x,y)} - \mu_{r3l(x,y)}\,\mathrm{sgn}\left(\dot{\varphi}_{(x,y)}\right)\sin\varphi_{(x,y)} + \tan\frac{\varphi_{(x,y)}}{2}\sin\varphi_{(x,y)}} \tag{9}$$

It should be mentioned that $\mu_{r1l(x,y)}$, $\mu_{r2l(x,y)}$ and $\mu_{r3l(x,y)}$ actually are not constant and depend on the value of normal forces. In this study the following relations, obtained based on experimental study (Hosseini and Soroor, 2011), are used:

$$\mu_{r1l(x,y)} = \frac{(3e-8)N^2_{1l(x,y)} + 0.006N_{1l(x,y)} + 7.801}{N_{1l(x,y)}} \tag{10}$$

$$\mu_{r2l(x,y)} = \frac{(3e-8)N^2_{2l(x,y)} + 0.006N_{2l(x,y)} + 7.801}{N_{2l(x,y)}} \tag{11}$$

$$\mu_{r3l(x,y)} = \frac{(3e-8)N^2_{3l(x,y)} + 0.006N_{3l(x,y)} + 7.801}{N_{3l(x,y)}} \tag{12}$$

The values of P_l (l=1 to 9) are the axial forces of nine columns of the building at foundation level above isolators, each one is the resultants of vertical forces impose to the column because of the act of lateral seismic forces which are obtained by the following equation for both x and y directions:

$$p_{(x,y)} = \frac{H\ddot{u}_{g(x,y)}}{3L_{(x,y)}}\sum_{i=1}^{n} i\times m_i \tag{13}$$

Calculating p_x and p_y values for each column using Eq. (13) the P_l values are as follows:

$$P_1 = -\left(p_x + p_y\right) \quad , \quad P_2 = -p_y \quad , \quad P_3 = p_x - p_y \tag{14}$$

$$P_4 = -p_x \quad , \quad P_5 = 0 \quad , \quad P_6 = p_x \tag{15}$$

$$P_7 = p_y - p_x \quad , \quad P_8 = p_y \quad , \quad P_9 = p_x + p_y \tag{16}$$

By substituting the energy and work terms in Eq. (1) from Eqs. (2) to (4) and performing the required mathematical elaborations (Mahmoudkhani, 2013) the set of Lagrange equations of motion for the bi-directional oscillations of the UR-OPRCB isolator can be written as:

$$\begin{aligned}
&4m_b(R-r)^2\left(\ddot{\theta}_x\cos^4\frac{\theta_x}{2} - \dot{\theta}_x^2\cos^3\frac{\theta_x}{2}\sin\frac{\theta_x}{2}\right) + m_t(R-r)^2\left(\ddot{\theta}_x\sin^2\theta_x + \dot{\theta}_x^2\sin\theta_x\cos\theta_x + \frac{g\sin\theta_x}{R-r}\right)\\
&+(k_{bx}+k_{1x})(R-r)^2(1+\cos\theta_x)(\theta_x+\sin\theta_x) - k_{1x}(R-r)(1+\cos\theta_x)u_{1x}\\
&+4(c_{bx}+c_{1x})(R-r)^2\dot{\theta}_x\cos^4\frac{\theta_x}{2} - 2c_{1x}(R-r)\cos^2\frac{\theta_x}{2}\dot{u}_{1x}\\
&= -m_b\ddot{u}_{gx}(R-r)(1+\cos\theta_x) - m_t\ddot{v}_g(R-r)\sin\theta_x - \sum_{l=1}^{9}\left[heaviside(N_{2lx})\,\mathrm{sgn}(\dot{\theta}_x)F_{rlx}(R-r)\right]\\
&+\sum_{l=1}^{9}\left[\frac{heaviside(-N_{2lx})\,\mathrm{sgn}(\dot{\varphi}_x)F_{rulx}(R-r)(1+\cos\theta_x)}{\cos\varphi_x}\right]
\end{aligned} \tag{17}$$

$$4m_b(R-r)^2\left(\ddot{\theta}_y\cos^4\frac{\theta_y}{2}-\dot{\theta}_y^2\cos^3\frac{\theta_y}{2}\sin\frac{\theta_y}{2}\right)+m_t(R-r)^2\left(\ddot{\theta}_y\sin^2\theta_y+\dot{\theta}_y^2\sin\theta_y\cos\theta_y+\frac{g\sin\theta_y}{R-r}\right)$$
$$+\left(k_{by}+k_{1y}\right)(R-r)^2(1+\cos\theta_y)(\theta_y+\sin\theta_y)-k_{1y}(R-r)(1+\cos\theta_y)u_{1y}$$
$$+4\left(c_{by}+c_{1y}\right)(R-r)^2\dot{\theta}_y\cos^4\frac{\theta_y}{2}-2c_{1y}(R-r)\cos^2\frac{\theta_y}{2}\dot{u}_{1y}$$
$$=-m_b\ddot{u}_{gy}(R-r)(1+\cos\theta_y)-m_t\ddot{v}_g(R-r)\sin\theta_y-\sum_{l=1}^{9}\left[heaviside(N_{2ly})\operatorname{sgn}(\dot{\theta}_y)F_{rly}(R-r)\right]$$
$$+\sum_{l=1}^{9}\left[\frac{heaviside(-N_{2ly})\operatorname{sgn}(\dot{\theta}_y)F_{ruly}(R-r)(1+\cos\theta_y)}{\cos\theta_y}\right] \quad (18)$$

$$m_1\ddot{u}_{1x}+k_{1x}\left(u_{1x}-(R-r)(\theta_x+\sin\theta_x)\right)-k_{2x}(u_{2x}-u_{1x})+c_{1x}\left(\dot{u}_{1x}-2(R-r)\dot{\theta}_x\cos^2\frac{\theta_x}{2}\right)$$
$$-c_{2x}(\dot{u}_{2x}-\dot{u}_{1x})=-m_1\ddot{u}_{gx} \quad (19)$$

$$m_1\ddot{u}_{1y}+k_{1y}\left(u_{1y}-(R-r)(\theta_y+\sin\theta_y)\right)-k_{2y}(u_{2y}-u_{1y})+c_{1y}\left(\dot{u}_{1y}-2(R-r)\dot{\theta}_y\cos^2\frac{\theta_y}{2}\right)$$
$$-c_{2y}(\dot{u}_{2y}-\dot{u}_{1y})=-m_1\ddot{u}_{gy} \quad (20)$$

$$m_i\ddot{u}_{ix}+k_{ix}\left(u_{ix}-u_{(i-1)x}\right)-k_{(i+1)x}\left(u_{(i+1)x}-u_{ix}\right)+c_{ix}\left(\dot{u}_{ix}-\dot{u}_{(i-1)x}\right)-c_{(i+1)x}\left(\dot{u}_{(i+1)x}-\dot{u}_{ix}\right)=-m_i\ddot{u}_{gx} \quad (21)$$

$$m_i\ddot{u}_{iy}+k_{iy}\left(u_{iy}-u_{(i-1)y}\right)-k_{(i+1)y}\left(u_{(i+1)y}-u_{iy}\right)+c_{iy}\left(\dot{u}_{iy}-\dot{u}_{(i-1)y}\right)-c_{(i+1)y}\left(\dot{u}_{(i+1)y}-\dot{u}_{iy}\right)=-m_i\ddot{u}_{gy} \quad (22)$$

NUMERICAL ANALYSIS OF SEISMIC RESPONSES OF CONSIDERED BUILDINGS

Using the system of the partial differential equations of motion, the seismic response of 3-, 6-, and 9-story building with the aforementioned plan, with span length of 5m in both directions, and story height of 3m, subjected to a set of near-source earthquake 3-component acceleration records, given in Table 1, have been calculated using Runge-Kutta-Nyström method (Collatz, 1966).

Table 1. Set of 3-component records of the near-source earthquakes

Record	PGA (g)				Dominant Frequency (Hz)		
	Vertical		In x direction	In y direction	Vertical	In x direction	In y direction
	Upward	Downward					
NGA0183	0.40	0.44	0.60	0.45	0.25	0.74	0.27
NGA0184	0.71	0.49	0.48	0.35	0.25	0.73	0.37
NGA0230	0.39	0.35	0.44	0.42	1.61	1.72	1.49
NGA0540	0.47	0.36	0.61	0.49	1.85	2.78	1.92
NGA0741	0.51	0.39	0.53	0.48	2.78	2.13	1.52
NGA0752	0.54	0.53	0.53	0.44	4.76	0.70	1.49
NGA0766	0.29	0.21	0.37	0.32	2.44	2.50	0.70
NGA0802	0.35	0.39	0.51	0.32	0.79	0.55	0.29
NGA1505	0.49	0.33	0.57	0.46	0.28	0.40	0.53

The amount of story mass used in the considered buildings was 59184.34 kg. The damping coefficients were calculated by assuming a value of 5% for the damping ratios of the first two modes of the buildings in each case. The values of effective stiffness and damping coefficient for various stories of the considered buildings are given in Table 2. Fig. 16 shows a sample of response histories, which relates to the axial force of a corner column of 3-story building subjected to NGA0180 record.

Table 2. Effective story stiffness (N/m) and damping coefficient (N.sec/m) of the considered buildings

Stories	3-story building		6-story building		9-story building	
1, 2 and 3	K_e=2.98e8	C_e=9.44e5	K_e=4.47e8	C_e=2.25e6	K_e=5.96e8	C_e=3.93e6
4, 5 and 6	-	-	K_e=2.98e8	C_e=1.50e6	K_e=4.47e8	C_e=2.95e6
7, 8 and 9	-	-	-	-	K_e=2.98e8	C_e=1.97e6

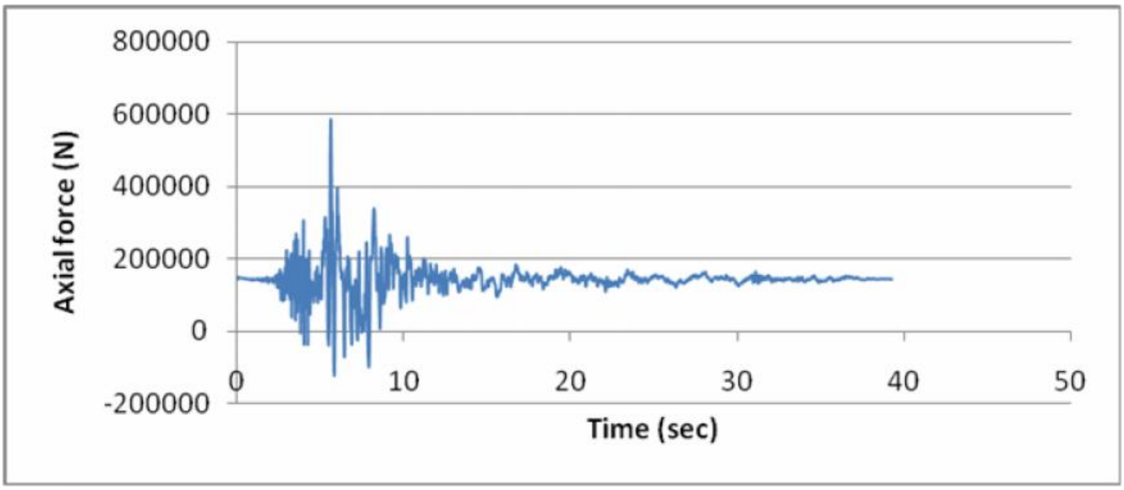

Figure 3. Axial force time history of a corner column of 3-story building subjected to NGA0180 record

It can be seen in Fig. 3 that in some instances during the strong ground motion the corner column has experienced uplift forces, which its maximum is around 120,000 N or almost 12 tonf. Tables 3 to 5 show the peak values of drift and acceleration responses in the considered buildings subjected to the employed earthquakes.

It can be seen in Tables 3 to 5 that using the UR-OPRCB isolators results in respectively 32% and 62% reduction in drift and acceleration responses, in average, in case of 3-story building. These reduction factors are in average 15% and 59% in case of 6-story building and 11% and 55% in case of 9-story building. It is worth mentioning that without uplift restrainers, in several cases, like the case shown in Fig. 3, the OPRCB isolator could not act properly due to uplift, while with using the uplift restrainers the isolator has performed quite well in the whole duration of the seismic excitation.

Table 3. Peak values of drift and acceleration responses in the 3-story building

Record	Maximum Drift		Maximum Acceleration (m/s^2)		Ratio of drift values (Isolated to Fixed Base)	Ratio of acceleration values (Isolated to Fixed Base)
	Fixed Base	Isolated	Fixed Base	Isolated		
NGA0183	0.00592	0.00370	13.17	5.40	0.63	0.41
NGA0184	0.00565	0.00415	12.03	5.41	0.73	0.45
NGA0230	0.00701	0.00437	14.77	4.73	0.62	0.32
NGA0540	0.00928	0.00496	16.37	4.42	0.53	0.27
NGA0741	0.00550	0.00425	12.33	3.58	0.77	0.29
NGA0752	0.00758	0.00425	11.66	4.78	0.56	0.41
NGA0766	0.00496	0.00397	8.67	2.86	0.80	0.33
NGA0802	0.00609	0.00451	13.52	5.95	0.74	0.44
NGA1505	0.00479	0.00377	7.68	3.61	0.79	0.47

Table 4. Peak values of drift and acceleration responses in the 6-story building

Record	Maximum Drift		Maximum Acceleration (m/s^2)		Ratio of drift values (Isolated to Fixed Base)	Ratio of acceleration values (Isolated to Fixed Base)
	Fixed Base	Isolated	Fixed Base	Isolated		
NGA0183	0.00652	0.00480	14.50	6.38	0.74	0.44
NGA0184	0.00612	0.00577	13.03	5.99	0.94	0.46
NGA0230	0.00659	0.00664	13.89	5.14	1.01	0.37
NGA0540	0.00981	0.00658	17.30	5.36	0.67	0.31
NGA0741	0.00592	0.00481	13.28	3.98	0.81	0.30
NGA0752	0.00816	0.00550	12.55	5.52	0.67	0.44
NGA0766	0.00590	0.00552	10.31	3.61	0.94	0.35
NGA0802	0.00644	0.00685	14.29	6.86	1.06	0.48
NGA1505	0.00610	0.00501	9.78	4.99	0.82	0.51

Table 5. Peak values of drift and acceleration responses in the 9-story building

Record	Maximum Drift		Maximum Acceleration (m/s^2)		Ratio of drift values (Isolated to Fixed Base)	Ratio of acceleration values (Isolated to Fixed Base)
	Fixed Base	Isolated	Fixed Base	Isolated		
NGA0183	0.00732	0.00621	15.23	6.85	0.85	0.45
NGA0184	0.00688	0.00806	13.68	6.70	1.17	0.49
NGA0230	0.00741	0.00687	14.58	5.69	0.93	0.39
NGA0540	0.01102	0.00916	16.60	6.14	0.83	0.37
NGA0741	0.00666	0.00632	13.94	5.30	0.95	0.38
NGA0752	0.00917	0.00731	11.85	5.57	0.80	0.47
NGA0766	0.00663	0.00516	10.83	4.55	0.78	0.42
NGA0802	0.00723	0.00678	13.93	7.52	0.94	0.54
NGA1505	0.00686	0.00535	10.27	5.65	0.78	0.55

CONCLUSIONS

Based on the numerical results of this study, obtained from time history analysis of 3- to 9-strory regular buildings (with aspect ratios of around 1.0 to 3.0), equipped with UR-OPRCB isolators, it can be concluded that:

- Using UR-OPRCB isolators can reduce the maximum story drift values around 20%, and the maximum absolute acceleration values around 60% in average.
- In case of some earthquake records slight increase in the maximum story drift values is observed which can be due to the relatively high energy of those earthquakes in the range of long periods, particularly around 2.0 seconds (period of the isolated systems).

Finally, it should be noted that the U-shaped restrainers used in this study have been investigated only based on numerical modeling and analysis. To get more reliable results in this regard, conducting some experimental studies would be much helpful.

REFERENCES

Collatz L (1966) The numerical treatment of differential equations, 3rd Ed., Springer-Verlag, New York

Chung LL, Yang CY, Chen HM and Lu LY (2009) Dynamic behavior of nonlinear rolling isolation system, *Structural Control and Health Monitoring*, 16(1): 32-54

Hosseini M and Soroor A (2011) Using Orthogonal Pairs of Rollers on Concave Beds (OPRCB) as a Base Isolation System—Part I: Analytical, Experimental and Numerical Studies of OPRCB Isolators, The *Structural Design of Tall and Special Buildings*, 20(8): 928-950

Hosseini M and Soroor A (2013) Using Orthogonal Pairs of Rollers on Concave Beds (OPRCB) as a Base Isolation System—Part II: Application to Multi-Story and Tall Buildings, *The Structural Design of Tall and Special Buildings*, 22(2): 192-216

Jangid RS (1995) Seismic response of structure isolated by free rolling rods, *European Earthquake Engineering*, 9: 3-11

Londhe YB and Jangid RS (1999) Dynamic response of structures supported on elliptical rolling rods, *Structural Engineering Earthquake Engineering*, 16: 1s-10s

Mahmoudkhani S (2013) Protection of the Orthogonal Pairs of Rollers in Concave Beds (OPRCB) Isolation System against Uplift Forces, M.Sc. Thesis, Earthquake Engineering Department, Science and Research Branch of the Islamic Azad University, Tehran, Iran

Ou YC, Song J and Lee GC (2010) A parametric study of seismic behavior of roller seismic isolation bearings for highway bridges, *Earthquake Engineering & Structural Dynamics*, 39(5): 541-559

Tsai MH, Wu SY, Chang KC and Lee GC (2007) Shaking table tests of a scaled bridge model with rolling-type seismic isolation bearings, *Engineering structures*, 29(5): 694-702

Wang, SJ, Hwang JS, Chang KC, Shiau CY, Lin WC, Tsai MS, Hong JX and Yang YH (2014) Sloped multi-roller isolation devices for seismic protection of equipment and facilities, *Earthquake Engineering & Structural Dynamics*, 43(10): 1443-1461